Environmental Science and Pollution Research (2020) 27:28091–28103
https://doi.org/10.1007/s11356-020-09127-y

RESEARCH ARTICLE

Adsorption kinetics of methyl orange from water by pH-sensitive poly(2-(dimethylamino)ethyl methacrylate)/nanocrystalline cellulose hydrogels

Seyedeh-Arefeh Safavi-Mirmahalleh[1,2] · Mehdi Salami-Kalajahi[1,2] · Hossein Roghani-Mamaqani[1,2]

Received: 10 September 2019 / Accepted: 29 April 2020 / Published online: 14 May 2020

Abstract

A series of hydrogel nanocomposites was fabricated by in situ polymerization of 2-(dimethylamino)ethyl methacrylate (DMAEMA) in presence of different amounts of (amine- and alkyl-modified) nanocrystalline cellulose (NCC). Modification and nanocomposites properties were proved by different analysis methods such as Fourier-transform infrared spectroscopy (FT-IR), dynamic light scattering (DLS), and field emission scanning electron microscopy (FE-SEM). The new hydrogel nanocomposites were applied for removing methyl orange (MO) used as anionic dye and presented in process water at different pH values. The effects of the fabrication process such as modification and content of NCC, contact time, and pH value on swelling ratio (SR), and equilibrium adsorption kinetics were studied. Results showed that the swelling ratio of PDMAEMA-based nanocomposites varied with the different types of nanoparticles showing the significant effect of the modification process. The MO adsorption into the hydrogel nanocomposites was affected by intermolecular and electrostatic interactions between functional groups of hydrogel and dye. The adsorption capacity decreased at high pH value, and it was significantly affected type of nanoparticles introduced into the hydrogel network. The addition of unmodified NCC did not affect adsorption kinetics significantly. Finally, adsorption kinetics was investigated by pseudo-first-order, pseudo-second-order and intraparticle diffusion models where pseudo-first-order model showed the best correlation with experimental results.

Keywords Nanocrystalline cellulose · Poly(2-(dimethylamino)ethyl methacrylate) · Nanocomposite hydrogels · Swelling ratio · Adsorption kinetic · Methyl orange

Introduction

A large amount of synthetic dyes are used in different industries such as textile (Patil et al. 2010), printing (Seema et al. 2018), cosmetics, food (Guerra et al. 2018), paper making (Blus et al. 2014), etc. Anionic dyes are applied mostly because of their excellent color fastness, bright colors, etc. However, dyes are usually toxic and harmful to humans and environment and need to be removed from the effluents. Various treatments are applied for dye removal such as coagulation-flocculation (Panswed and Wongchaisuwan 1986), oxidation (Malik and Saha 2003), membrane separation (Ciardelli et al. 2001), electrochemical processes (de Paiva et al. 2018), etc. Among these, adsorption is a widely-used method because of its low operating cost, capability to operate at very low concentrations, simple design and easy technical access (Cheng et al. 2016; Abousalman-Rezvani et al. 2019a). Activated carbon (Mezohegyi et al. 2012), inorganic-organic hybrid materials (García et al. 2014), industrial byproducts and wastes (Ahmad et al. 2009), and hydrogels (Soleimani et al. 2018) are the most used adsorbents for removal of different dyes.

It is well-known that ionic hydrogel adsorbents can be used for removal of oppositely charged dyes, ions, and heavy metals

Responsible editor: Angeles Blanco

Electronic supplementary material The online version of this article (https://doi.org/10.1007/s11356-020-09127-y) contains supplementary material, which is available to authorized users.

✉ Mehdi Salami-Kalajahi
m.salami@sut.ac.ir

✉ Hossein Roghani-Mamaqani
r.mamaghani@sut.ac.ir

[1] Faculty of Polymer Engineering, Sahand University of Technology, P.O. Box 51335-1996, Tabriz, Iran

[2] Institute of Polymeric Materials, Sahand University of Technology, P.O. Box 51335-1996, Tabriz, Iran

(Kaşgöz and Durmus 2008; Bekiari et al. 2008; Atta et al. 2012; Lu et al. 2015; Abousalman-Rezvani et al. 2019b). Hydrogels adsorb materials from aqueous solutions and keep them dissolved and swell up by water absorption (Abdollahi et al. 2016; Nikravan et al. 2018) by making hydrogen bonding with water (Fallahi-Samberan et al. 2019) or electrostatic interactions (Modarresi-Saryazdi et al. 2018; Dehghani et al. 2019). The amount of absorbed water can be controlled by variation of pH or temperature (Liu et al. 2010; Balea et al. 2017).

Introduction of natural materials into structure of hydrogels affects swelling properties and therefore adsorption capacity. Among them, those based on nontoxic and biodegradable polysaccharides are one of the most attractive ones due to their unique properties like hydrophilicity, ecofriendly behavior, and biodegradation (Abdeen and Mohammad 2014; Sharma et al. 2015). Cellulose as naturally renewable and the most available polysaccharide has unique mechanical and physical properties (Khadivi et al. 2019a,b), and due to its hydroxyl groups, it can be modified by different compounds (Bayramoglu et al. 2012; Zhou et al. 2014) to improve water absorption and dye adsorption (Ibrahim et al. 2007). Pei et al. (2013) reported fabrication of surface-quaternized cellulose nanofibrils to be used for removal of Congo red as anionic dye. Stanciu and Nichifor (2019) synthesized dextran hydrogel with quaternary ammonium pendent groups and used it in removal of methyl orange (MO) as anionic dyes. Haque et al. (2011) prepared an iron terephthalate as metal-organic frameworks (MOFs) and applied it for the adsorption of MO and methylene blue (MB) as anionic and cationic dyes respectively. Fang et al. (2016) synthesized a high-capacity cationic hydrogel adsorbent (CHA) for adsorption of Acid Black. Zhao et al. (2012) produced semiIPN hydrogel composites by photopolymerization of poly(ethylene glycol) and acrylamide (AAm) in presence of chitosan (CS) and used them for dye adsorption studies. Chatterjee et al. (2016) synthesized chitosan-based hydrogel beads and studied the effect of alkali treatment on morphology, adsorption ability, and surface chemistry. Balea et al. (2019) combined cellulose nanofibers with chitosan for a successfully removal of flexographic inks (copper phthalocyanine blue, carbon black, and diarylide yellow), and Sanchez-Salvador et al. (2018) showed the dye removal effect of nanocellulose-graft-chitosan polymers. Zhang et al. (2017) synthesized a magnetic cellulose/Fe_2O_3 hydrogels by sol-gel transition method and used it as adsorbent of MO. Chen et al. (2017) prepared nitrogen-doped TiO_2/Q-NFC hybrid cryogels by one pot hydrothermal treatment method and their MO adsorption/photodegradation properties were characterized. Li et al. (2017) prepared a cationic absorbent polyepichlorohydrin-ethylenediamine hydrogel for removal of dyes and insoluble oil from wastewater. Karthika and Vishalakshi (2015) studied the grafting of DMAEMA on Gellan gum and its adsorption capacity for MO. Liu et al. (2015a, b) synthesized poly(DMAEMA-co-AA) hydrogels as adsorbent of anionic and cationic dyes. Salama et al. prepared an adsorbent based on carboxymethyl cellulose (CMC) for MO removal from aqueous solution. For this aim, DMAEMA was grafted onto backbone of CMC. Then, the effect of solution pH, contact time, and dye concentration on the adsorption behavior was studied (Salama et al. 2015). Zheng et al. (2018) synthesized a composite film using chitosan and dialdehyde microfibrillated cellulose nano fibrils by solvent-casting method for adsorbtion of Congo red from aqueous solution. Lin et al. (2016) prepared an adsorbent based on cross-linked CMC by grafting of dimethyldiallylammonium chloride (DMDAAC), and its adsorption properties on MO and MB dyes were investigated. Kono et al. (2016) synthesized a series of cationic cellulose hydrogels (CCGs) by crosslinking reaction with PEGDE as a crosslinking agent, and their adsorption capacity for three types of anionic dyes, AR13, AB92, and AR112 was investigated. Oladipo et al. (2014) prepared a semiIPN composite hydrogel from cellulose-graft-polyacrylamide and HAP where adsorption behavior for RB2 was investigated. Tu et al. (2017) prepared the chitosan/REC/cellulose composite hydrogels for removal of Congo red from aqueous solution in different adsorption conditions. Kono (2015) fabricated a cellulose polyampholyte hydrogels and the adsorption capacity of the hydrogels was investigated for three anionic dyes AR9, AR13, and AB92.

In current work, NCC is modified by (3-amino)propyltriethoxysilane (APTES) and hexadecyltrimethoxysilane (HMTS) to prepare ANCC and HNCC respectively to investigate the effect of surface groups on swelling and dye removal behaviors of nanocomposite hydrogels. Crosslinked PDMAEMA/NCC hydrogels containing various amounts of (modified) NCC are fabricated by in situ polymerization and used as MO adsorbent. Due to pH-sensitive swelling properties of the hydrogels, dye adsorption properties are studied at different pH values. Finally, adsorption kinetics of MO is investigated.

Experimental methods

Materials

2-(dimethylamino)ethyl methacrylate (DMAEMA, Aldrich, 98%) was distilled and stored at 0 °C. Microcrystalline cellulose (MCC, Sigma-Aldrich, 98%), sulfuric acid (H_2SO_4, Merck, 98%), (3-aminopropyl)triethoxysilane (APTES, Sigma-Aldrich, 99%), hexadecyltrimethoxysilane (HDTMS, Sigma-Aldrich, ≥ 85%), N,N'-methylenebis(acrylamide) (MBA, Sigma-Aldrich, 99%), potassium persulfate (KPS, Merck, 99%), azobisisobutyronitrile (AIBN, Aldrich, 98%), methyl orange (MO, Merck, %), sodium hydroxide (NaOH, Merck, ≥ 97), and ethanol (Kimia Alcohol Zanjan, 96%) were used as received.

Preparation and modification of NCC

NCC rods (100–200 nm in length and 10–20 nm in diameter, Fig. S1) were prepared by acid hydrolysis of MCC (10–50 μm in length and 10–25 μm in diameter, Fig. S1) as reported in literature (Golshan et al. 2017; Safavi-Mirmahalleh et al. 2019). In modification step, NCC (0.5 g) was sonicated (Hielscher UP400, 30 min at room temperature) in ethanol (50 mL) and after that, modifier was added dropwise (2 mL, 8.5 mmol APTES, and 5.13 mmol HDTMS). Reaction was continued for 3 h at 60 °C under nitrogen atmosphere. Obtained suspension was centrifuged (Hettich Universal 320) at 10000 rpm and washed with water/ethanol three times. The final product (ANCC for APTES and HNCC for HDTMS) was then freeze-dried (Dena Vacuum FD-5010-BT) overnight.

Synthesis of PDMAEMA-based nanocomposite hydrogels

To synthesize nanocomposite hydrogels, DMAEMA was crosslinked by MBA in presence of different amount of (modified) NCCs (1.0–3.0 wt. %). To this end, NCC was ultrasonically (Hielscher UP400, 30 min at room temperature) dispersed in water, and then, DMAEMA was added to the mixture where a homogenous media was obtained using a magnetic stirrer. After that MBA (0.26 g, 1.7 mmol) in 5-mL water was added. After rising temperature to 60 °C, KPS (0.06 g, 0.2 mmol) was added, and reaction was completed after 24 h under nitrogen atmosphere. A same procedure was performed for modified NCCs (ANCC and HNCC). The samples were washed with distilled water for 3 days via dialysis method, and then final product was dried in vacuum at 50 °C. HNCC containing hydrogels were prepared in ethanol due to dispersibility problems of HNCC in water. Nanocomposite hydrogels were named HNCx, HACx, and HHCx for NCC, ANCC, and HNCC containing samples, respectively where x was the weight percentage of nanorods.

Investigation of swelling behavior

Gravimetry was used to study swelling behavior of nanocomposite hydrogels. After swelling of dried hydrogels at different pH values, sampling was performed at predetermined time intervals, and weighting was done after removing excess water on surface by Kleenex. The SR for each sample was

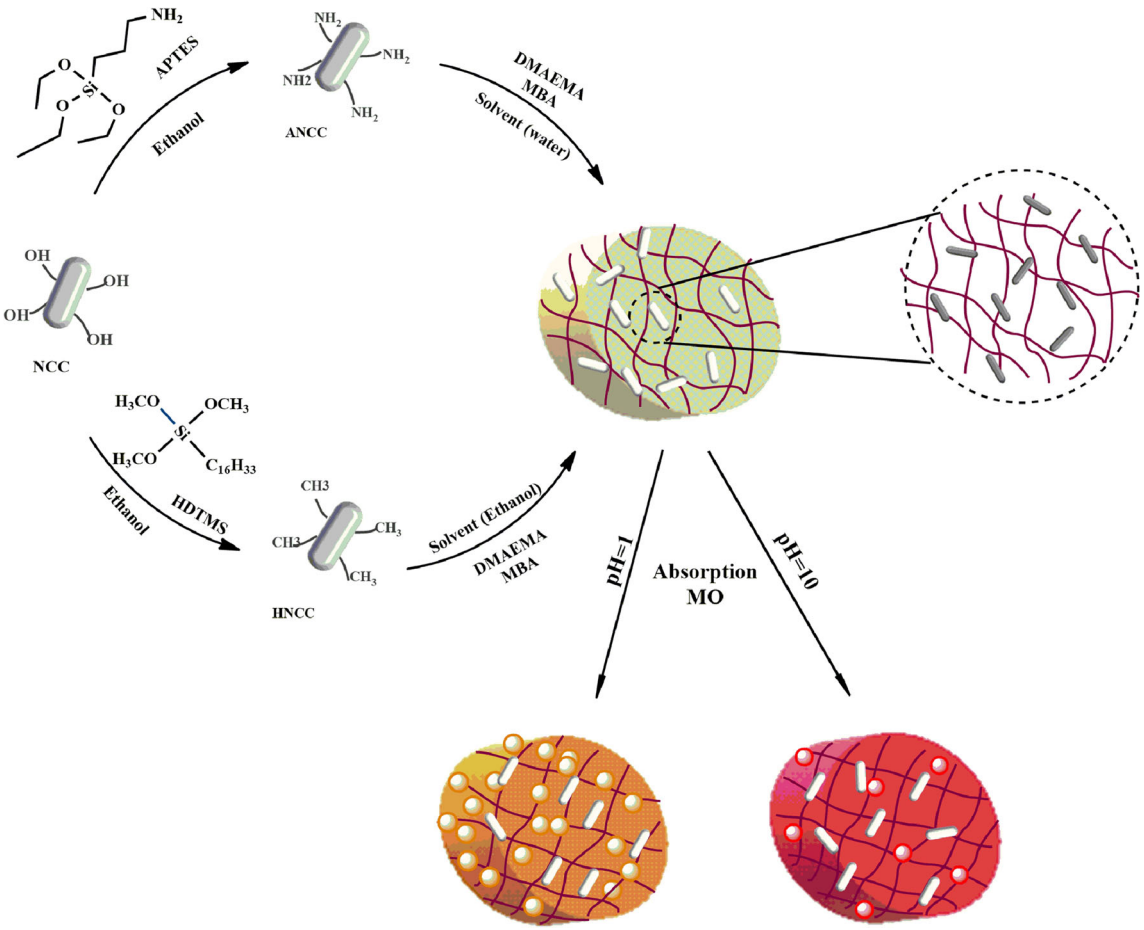

Scheme 1 Fabrication route and MO dye absorption of nanocomposite hydrogels

calculated based on dry and swollen weights (W_d and W_S) via Eq. (1) (Anirudhan and Rejeena 2012):

$$\mathrm{SR} = \frac{Ws - Wd}{Wd} \tag{1}$$

Investigation of adsorption behaviors

Dye uptake capacity of hydrogels was measured in aqueous solutions of MO at two pH values (acidic condition of pH = 1 where the hydrogels are fully-protonated and basic condition of pH = 10 where the hydrogels are deprotonated) at ambient temperature. Hydrogel (0.05 g) was soaked in MO solution (5 mg/L, 100 mL) and samples were taken out (1 mL) and replaced with fresh water during 6 days. Concentration of MO was evaluated at 468 nm for pH = 1 and 508 nm for pH = 10. The adsorption capacity (q_e, mg dye/g hydrogel) was obtained via Eq. (2) (Akkaya et al. 2009).

$$q_e = \frac{(Ci - Ce)\ V}{m} \tag{2}$$

C_i and C_e were initial and instantaneous concentrations of MO respectively considering V liter of solution and m g of hydrogel.

Characterization

Fourier transform infrared (FT-IR) spectroscopy was performed by means of a Bruker Tensor 27 FT-IR-spectrophotometer in the range between 500 and 4000 cm^{-1} with a resolution of 4 cm^{-1}. An average of 24 scans has been carried out for each sample. Particle size, particle size distribution, and zeta potential were measured by Malvern Instruments dynamic light scattering (DLS). The morphology of nanoparticles and nanocomposite hydrogels was observed by HITACHI S-4160 field emission scanning electron microscope (FE-SEM). The samples were coated with gold before FE-SEM characterization.

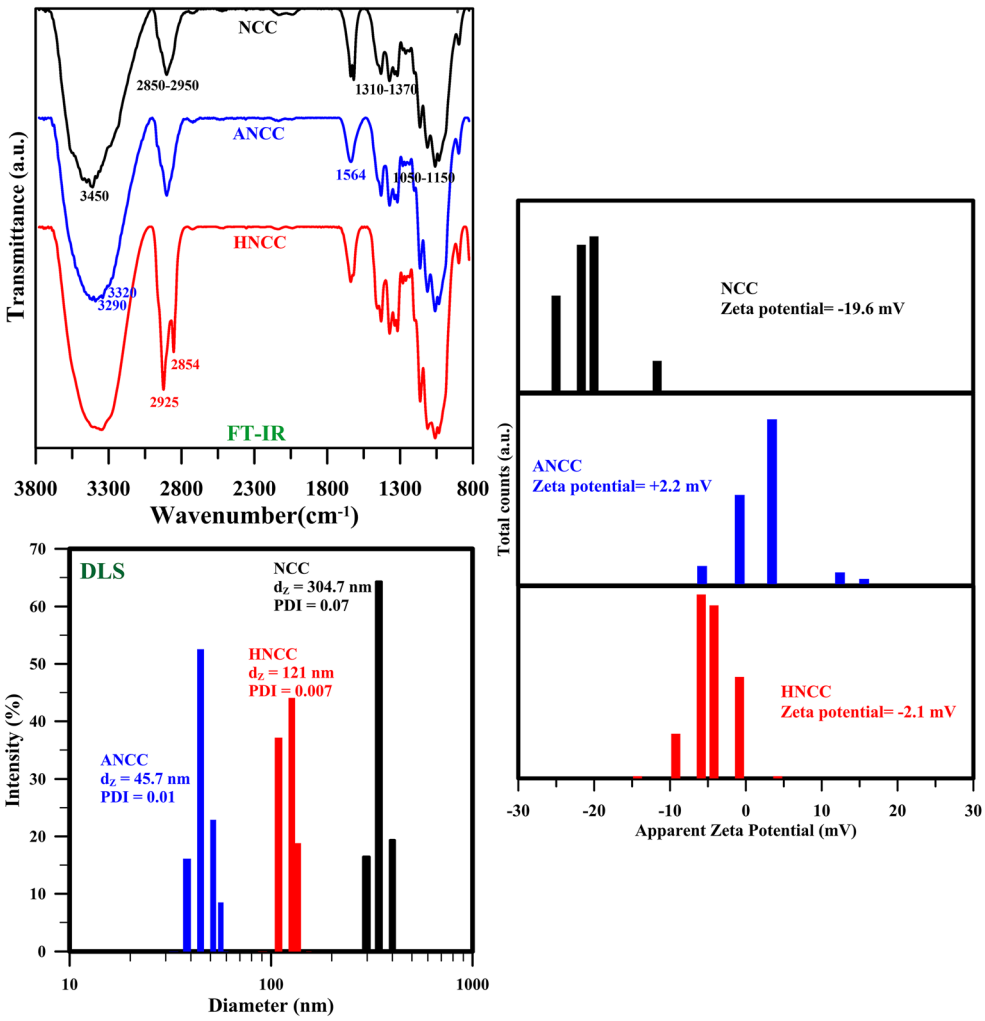

Fig. 1 FTIR, DLS, and zeta potential results of NCC, ANCC, and HNCC nanoparticles

Results and discussion

Herein, we have fabricated crosslinked PDMAEMA/NCCs hydrogels with various contents of nanoparticles. Then, they have been used as adsorbents of MO dye from water. The schematic of fabrication process and adsorption behavior of MO by hydrogels are presented in Scheme 1.

Synthesis and characterization of NCCs and nanocomposite hydrogels

FT-IR spectra of NCC, ANCC, and HNCC are shown in Fig. 1. Peak at 3450 cm^{-1} was due to hydroxyl groups participating in intracellular hydrogen bonding of cellulose (Haqani et al. 2017; Riazi et al. 2018) and peak at 2850–2950 cm^{-1} was ascribed to C–H stretching vibrations (Panahian et al. 2014a, b; Bidsorkhi et al. 2016). Peaks between 1310 and 1370 cm^{-1} originated from bending vibration of C–H and C–O groups in the polysaccharide rings of cellulose (Kargarzadeh et al. 2012) and peak at 1050–1110 cm^{-1} was ascribed to bending vibration of C–O–C. After modification, ANCC showed new peaks at 1564, 3290, and 3320 cm^{-1} due to stretching and bending vibrations of primary amines (Gao et al. 2009; Sharifzadeh et al. 2016). However, absorption peaks of Si–O–Si bonds were coincided on C–O bending modes of cellulose. HNCC showed symmetric and asymmetric vibrations of CH_2 groups at 2925 and 2854 cm^{-1} (Sarsabili et al. 2013; Luo et al. 2017). It is reported that size of nanoparticles could be affected after modification depending on both modifier length and interactions between modified nanoparticles (Banaei and Salami-Kalajahi 2015; Mahmoud et al. 2020). For example, change in surface plasmon resonance of gold nanoparticles results in increasing the particles size (Mazloomi-Rezvani et al. 2018) whereas there are some reports on reduction of size of different particles through modification (Pyatenko et al. 2009; Mahmoud et al. 2020). Thus, unmodified NCC and modified NCCs were analyzed by DLS at room temperature (Fig. 1). *Z* average particle size was reported 304.7 (polydispersity index (PDI) = 0.070), 45.7 (PDI = 0.01), and 121 nm (PDI = 0.007) for NCC, ANCC, and HNCC respectively. Modified nanoparticles showed smaller size than NCC because the breakdown of hydrogen bonding in NCC structure which prevents the agglomeration of NCCs. Larger particle size of HNCC than ANCC originated from hydrophobic interactions of HNCC as

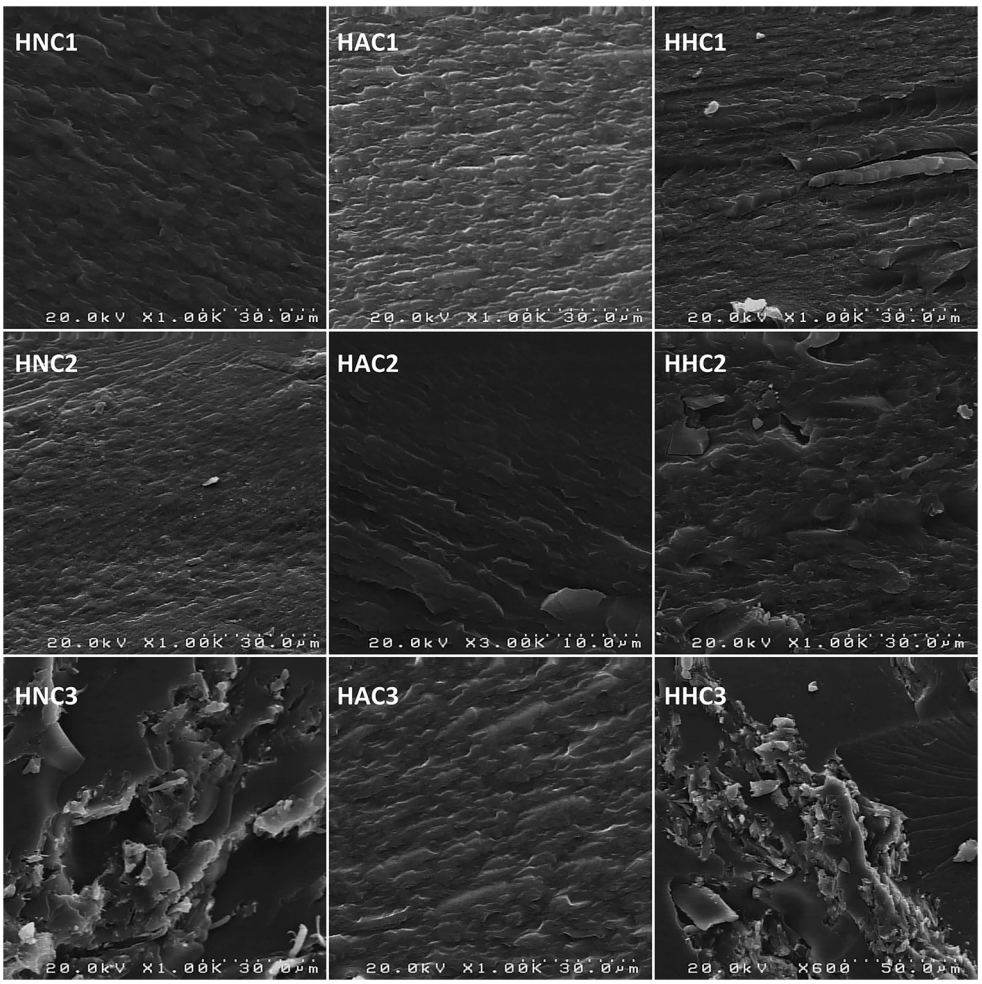

Fig. 2 FE-SEM images of PDMAEMA/(modified) NCC nanocomposite hydrogels

driving force of aggregation. Also, all samples showed narrow size distribution. Zeta potential of NCC, ANCC, and HNCC was obtained − 19.6, + 2.2, and − 2.1 mV respectively. Replacing hydroxyl groups with alkyl chain of HDTMS in HNCC resulted in smaller zeta potential whereas ANCC had a positive zeta potential originated from amines of APTES (Yamada et al. 2006).

FE-SEM images of HNC, HAC, and HHC hydrogels are shown in Fig. 2. This analysis was carried out on dried hydrogels due to difficulty of FE-SEM method in presence of water in the structure of hydrogel nanocomposites. According to results, all NCCs were aggregated in PDMAEMA matrix. The aggregation of nanoparticles might be related to a nanoparticles content, which led to interaction of neighbor nanoparticles in nanocomposite hydrogels (Ma et al. 2017). Meanwhile, the surface of nanocomposite hydrogels was rough because water diffused to structure of hydrogels and resulted in uneven surface morphology (Luo et al. 2018). Moreover, micrographs clearly illustrated that hydrogels morphology was dependent on the nanoparticles content and increasing NCC led to filling of structure and resulted in lower water penetration to structure (Bashir et al. 2017). However, HHC nanocomposite hydrogels had the most aggregated structure due to hydrophobic nature of HNCC surface, and dispersive forces were the most important driving force to form big agglomerations.

Swelling behavior of PDMAEMA/(modified) NCC nanocomposite hydrogels

Ability of swelling is one of the most important parameters to evaluate the properties of hydrogels. Higher swelling ratio means the ability of water absorption onto structure of a hydrogel. Herein, to study the effect of surface treatment of NCC on swelling ratio, different nanoparticles in neat or modified state are incorporated into the structure of PDMAEMA hydrogels. Figure 3 shows the swelling behavior of hydrogel nanocomposites containing 2 wt. % of (modified) NCCs. Generally, PDMAEMA-based hydrogels had very hydrophilic characteristics with high water adsorption capacity in acidic media. However, swelling ratio decreased continuously as pH increased. This was related to the protonation degree of

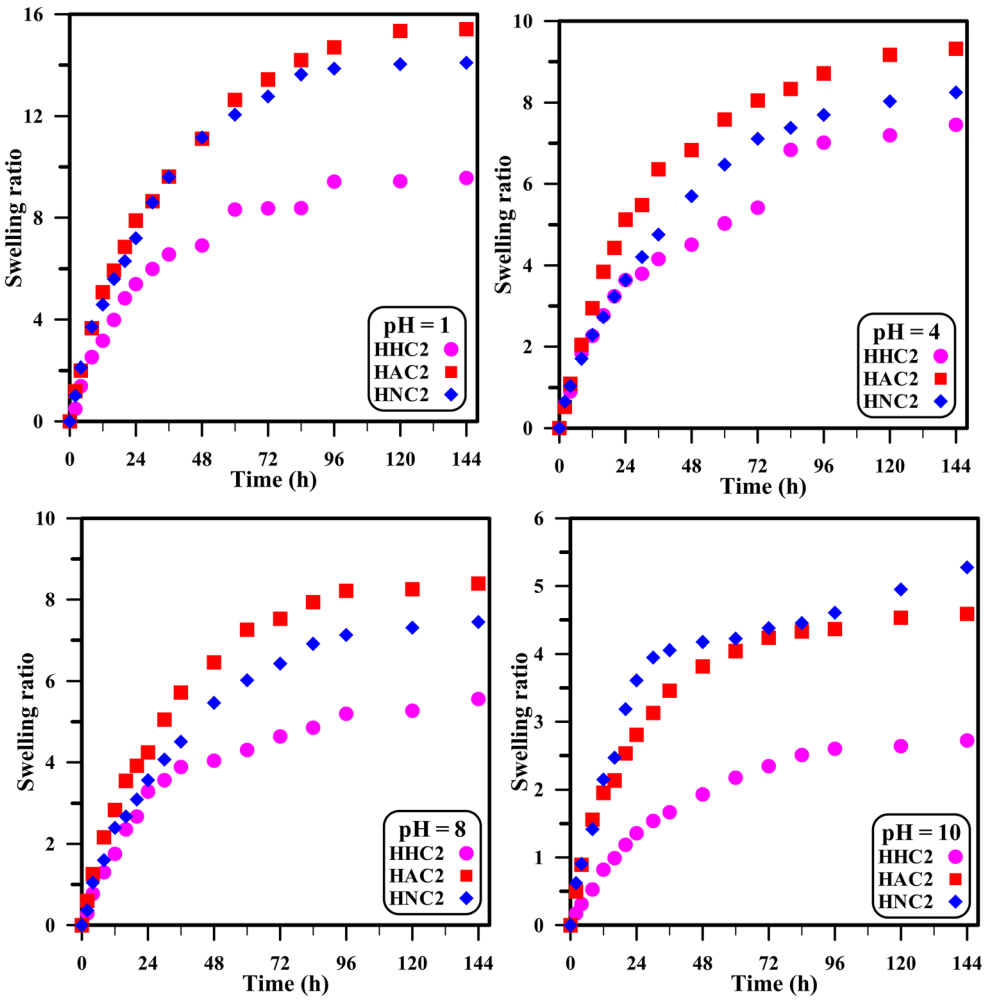

Fig. 3 SR of HNC2, HAC2, and HHC2 hydrogels at different pHs

dimethylamino (DMA) groups in structure of PDMAEMA. At acidic media, DMA groups were protonated which resulted in electrostatic repulsions between them (Dehghani et al. 2020). This caused swelling of hydrogel structure and diffusion of water molecules into the structure. However, by increasing pH value, DMA groups turned to half-protonated and deprotonated states which resulted in deswelling of hydrogels and decreasing water absorption (Noein et al. 2017). In hydrogel nanocomposites, HHC2 was the least swollen one because of HNCC's hydrophobic nature that led to less water absorption onto structure of hydrogels. Except pH = 10, HAC2 was the highest swollen sample because of its hydrophilic nature due to presence of primary amines on the surface. However, at pH = 10, HNC2 had a higher swelling ratio than HAC2. This might be due to deprotonation of amine groups on the surface of ANCC and electrostatic repulsions between negative charges on the surface of NCC which led to expansion of nanocomposite hydrogels and easy diffusion of water into structure of hydrogel.

Figure 4 represents the effect of content of NCCs on SR at two pH values (1 and 10). At pH = 1, PDMAEMA had strong hydrophilic characteristics, and NCC and ANCC as hydrophilic nanoparticles had no positive effect on nature of hydrogel hydrophilicity. Besides, they limited the expansion of 3D network by exertion of physical confinement on swelling of and filling hydrogel structure. As a result, swelling ratio was

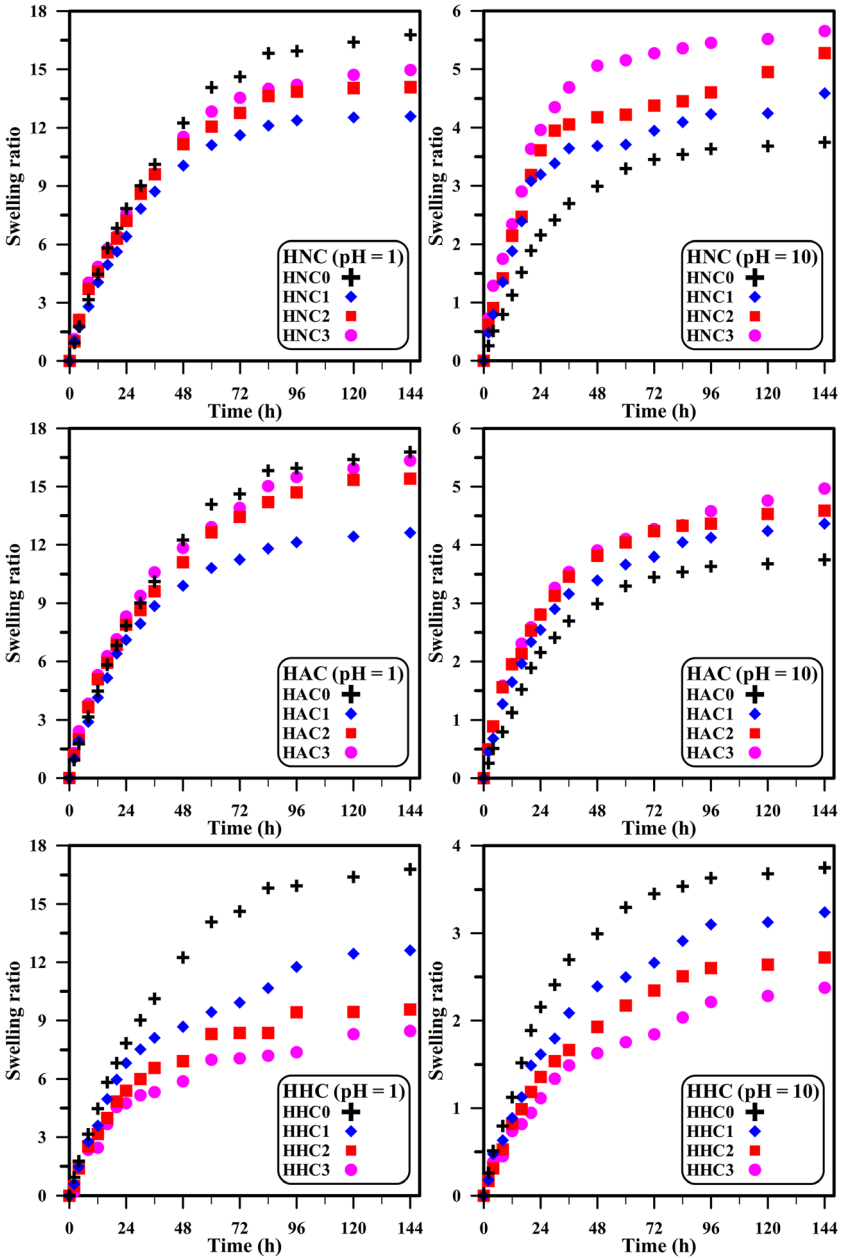

Fig. 4 Swelling ratio versus time for HNC, HAC, and HHC hydrogel nanocomposites at different pH values

decreased by adding NCC and ANCC nanoparticles. In HHC hydrogels, adding HNCCs led to dramatic decrease of SR due to hydrophobic structure of HNCC and structure filling of hydrogel with nanoparticles. This led to formation of more rigid structure and difficult water diffusion into network of hydrogels (Lim et al. 2017). At pH = 10, PDMAEMA electrostatic interactions were suppressed (Fallahi-Sambaran et al. 2018), and the effect of added nanoparticles became more predominant. Also, hydrogen bonding might exist among the free amino groups those limited the mobility of network chains and resulted in a dense hydrogel network; thus, a lower water absorption was exhibited. As a result, NCC and ANCC induced improvement in water absorption capacity of nanocomposite hydrogels due to their hydrophilic nature. Also, in the case of ANCC nanoparticle, free electron pair of the amino groups of ANCC nanoparticle could conjugate with carbonyl moieties in DMAEMA units. However, this interaction was weakened dramatically in acidic media due to protonation of tertiary amines (Hou et al. 2015). In HHC samples, even at pH = 10, higher amount of HNCC resulted in lower swelling ratio due to its hydrophobic surface nature that limited absorption of water molecules into hydrogel 3D structure.

Removal of MO by hydrogel nanocomposites

Dye removal by hydrogels is influenced by ionization degree of adsorptive molecule, charge of adsorbent, and dissociation of groups on functions of adsorbent (Tu et al. 2017). Conclusively, pH of dye solution is one of the most important parameters in adsorption process. At low pH, DMA groups of PDMAEMA are become ionized where electrostatic repulsions between positive DMA groups results in expansion of hydrogel. Besides, electrostatic interactions between positive DMA groups and negatively charged MO dye are become dominated. Thus, we chose these conditions according to pKa value of PDMAEMA (~ 8) where at pH = 1 all DMA moieties are protonated and positively charged (Mohammadi et al. 2017). However, at pH = 10 DMA groups become deprotonated and electrostatic interactions are disappeared. Thus, for more comparison, we reported the highest and lowest adsorption capacity. Also, according to swelling ratios, significant difference between swelling behaviors of hydrogels was observed between pH values of 1 and 10. Moreover, higher pH values were not tested because of hydrolysis of ester bonds in the structure of (meth)acrylates (Panahian et al. 2014b). Figure 5 represent the effect of pH of dye solution on adsorption capacity of hydrogels containing 2 wt. % NCCs where adsorption capacity of all samples was decreased at higher pH values. This originated from electrostatic interactions between deprotonated hydrogel structure at pHs higher than pK_a of PDMAEMA and MO. Beside this, deprotonation of DMA moieties at pH values higher than pK_a of DMAEMA resulted in shrinkage of hydrogel structure. Conclusively, MO molecules diffused more difficult into structure of hydrogel and decreased dye adsorption capacity was observed (Zhao et al. 2012). Modification of NCC also effected adsorption capacity and although HAC2 showed the highest adsorption capacity, no significant variation of adsorption capacity was obtained for different samples at pH = 10. This originated from low SR of hydrogels and difficult diffusion of MO into three-dimensional network. Also, at pH = 1, HAC2 and HHC2 nanocomposite showed the highest and the lowest adsorption capacity respectively. This could be explained by swollen structure of hydrogel nanocomposites as discussed in Figs. 3 and 4. Also, at pH = 1, ANCC had positive surface charge that could interact with anionic MO dye whereas HNCC and NCC had negative surface charge which discouraged dye adsorption into structure of hydrogel nanocomposites.

Figure 6 shows that introduction of (modified) NCC and increasing its content resulted in decreasing the adsorption capacity for all sample in acidic and alkali conditions. This originated from filling of structure and difficulty of MO diffusion from solution into hydrogel. Also, by increasing

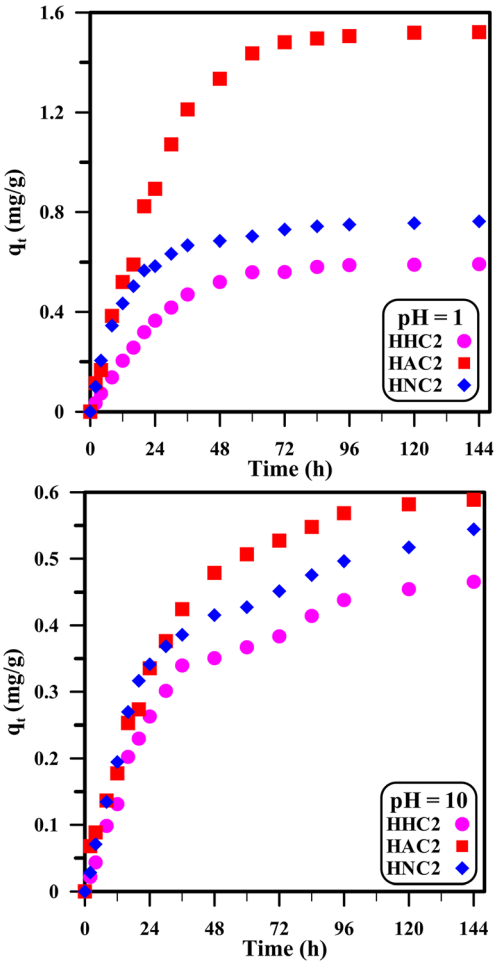

Fig. 5 Adsorption of MO for HNC2, HAC2, and HHC2 hydrogels vs. time at different pH of dye solution

pH from 1 to 10, adsorption capacity decreased from 1.64 to 0.95 mg/g for neat PDMAEMA hydrogel. This might be ascribed to the lower swelling ratio and also deprotonation of DMA groups at pH = 10 which results in less electrostatic interactions between PDMAEMA and MO as anionic dye. This coincides with the results of Salama et al. (2015) where by increasing pH from 2 to 6, the adsorption capacity was decreased from 193 to 135 mg/g due to more ionized groups at lower pH and electrostatic repulsions with adjacent groups. Also, incorporation of ANCC resulted in the least negative effect on adsorption capacity. ANCC had primary amine groups on its surface those could help adsorption of anionic MO dye; however, it exerted limitations on swelling of hydrogel during adsorption process. Lin et al. (2016) prepared a microsphere adsorbent based on CMC and DMDAAC for adsorption of anionic dyes where by increasing the amount of cationic monomer of DMDAAC, the adsorption capacity of microspheres was increased. NCC and HNCC affected adsorption capacity significantly because their surface charge was negative and electrostatic repulsions between them and dye resulted in lower adsorption of dye beside exertion of limitations on swelling of hydrogel. In this field, Liu et al. (2015a, b) synthesized the cellulose-based bioadsorbent that showed negative zeta potentials. Thus, the adsorption capacity was decreased due to augmentation electrostatic repulsions that coincides our result.

To investigate the adsorption kinetics of MO through different hydrogel nanocomposites, we used well-known

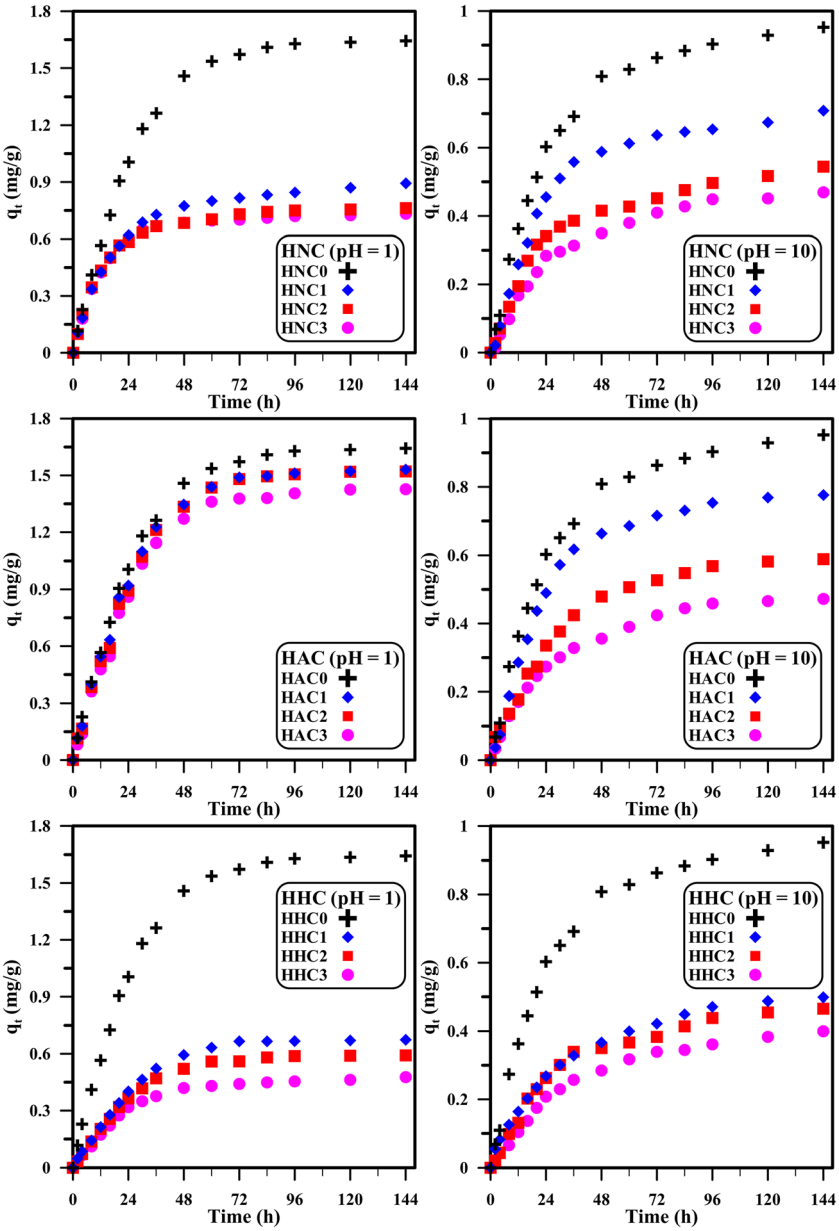

Fig. 6 Adsorption of MO by HNC, HAC, and HHC hydrogels versus time at different conditions

Table 1 Adsorption kinetic parameters of different models (k_1 (h^{-1}), k_2 (g mg^{-1} h^{-1}), and k_{id} (mg g^{-1} $h^{-1/2}$) for MO adsorption into hydrogel nanocomposites

Sample	pH = 1			pH = 10		
	k_1 (R^2)	k_2 (R^2)	k_{id} (R^2)	k_1 (R^2)	k_2 (R^2)	k_{id} (R^2)
HNC0	23.6 (0.9939)	12.8 (0.6425)	4.2 (0.9686)	25.8 (0.9948)	10.1 (0.8133)	8.1 (0.9892)
HNC1	19.9 (0.9950)	7.2 (0.9308)	7.6 (0.9743)	24.8 (0.9857)	7.6 (0.9109)	8.7 (0.9797)
HNC2	15.7 (0.9851)	4.4 (0.9469)	8.5 (0.9347)	23.2 (0.9870)	8.1 (0.9857)	12.5 (0.9595)
HNC3	13.7 (0.9994)	2.7 (0.8806)	8.2 (0.9322)	22.8 (0.9821)	8.1 (0.9750)	15.0 (0.9547)
HAC1	23.4 (0.9929)	12.4 (0.7189)	4.4 (0.9628)	23.9 (0.9914)	7.3 (0.8564)	7.9 (0.9844)
HAC2	22.9 (0.9810)	12.6 (0.6954)	4.5 (0.9570)	28.9 (0.9953)	7.8 (0.8485)	12.3 (0.9860)
HAC3	22.9 (0.9753)	10.5 (0.6444)	4.6 (0.9504)	30.4 (0.9876)	7.8 (0.9851)	15.9 (0.9856)
HHC1	24.4 (0.9970)	5.5 (0.6243)	9.3 (0.9902)	33.3 (0.9962)	9.4 (0.9767)	16.6 (0.9947)
HHC2	23.7 (0.9982)	4.8 (0.7050)	10.8 (0.9927)	30.4 (0.9856)	7.4 (0.9368)	14.6 (0.9775)
HHC3	22.9 (0.9948)	3.9 (0.7695)	12.9 (0.9849)	36.2 (0.9901)	8.4 (0.9563)	18.8 (0.9831)

mathematical adsorption models namely pseudo-first-order model (Eq. (3)), pseudo-second-order model (Eq. (4)), and intraparticle diffusion model (Eq. (5)) (Chen and Wang 2009; Melo et al. 2018; Bulut and Karaer 2015).

$$\ln(q_e - q_t) = \ln q_e - k_1 t \tag{3}$$

$$\frac{t}{q_t} = \frac{1}{q_e^2 k_2} + \frac{t}{q_e} \tag{4}$$

$$q_t = k_{id} t^{\frac{1}{2}} + c \tag{5}$$

where q_e and q_t are the extent of adsorbed dye on hydrogel at equilibrium state and any time respectively, and k_1, k_2, and k_{id} are constants. Calculated k_1, k_2, and k_{id} and also regression correlation coefficient (R^2) values are shown in Table 1. From the kinetic data, it could be concluded that pseudo-first-order kinetics model was the best model among data fitting at both pH = 1 and 10.

Conclusions

Herein, we prepared hydrogel nanocomposites with different modified and amount of NCCs to investigate the effect of surface chemistry of different modified NCCs on dye adsorption. Then, swelling and MO adsorption behaviors of hydrogel nanocomposites were studied at different pH values. HAC nanocomposites were the most swollen ones whereas HHC hydrogels had the least swelling ratio at pH values lower than pK_a of DMAEMA. However, HNC samples showed the highest SR at pH = 10 regarding filling of hydrogel structure and surface charge of nanoparticles. Moreover, lower pH resulted in protonation of DMA moieties of PDMAEMA, and their electrostatic repulsions caused higher SR of hydrogels. MO adsorption of hydrogel nanocomposites clarified that MO removal was influenced by the surface chemistry of NCCs, pH value of dye solution, and content of NCCs. As a main result, higher pH value resulted in lower adsorption capacities because DMAEMA DMA groups stayed on deprotonated form and could not do interaction with MO dye. However, HHC nanocomposite hydrogels had the lowest adsorption capacity due to lack of interacting functional groups on surface of HNCC and its negative surface charge. Also, kinetics studies showed that pseudo-first-order kinetics was the best model for predicting MO adsorption through all types of hydrogel nanocomposites.

Funding information This work was supported by the Iran National Science Foundation [grant number 97020973].

Data availability The raw/processed data required to reproduce these findings cannot be shared at this time as the data also form part of an ongoing study.

Compliance with ethical standards

Conflict of interest The authors declare that they have no conflict of interest.

References

Abdeen Z, Mohammad SG (2014) Study of the adsorption efficiency of an eco-friendly carbohydrate polymer for contaminated aqueous solution by organophosphorus pesticide. Open J Org Polym Mater 4: 16–28. https://doi.org/10.4236/ojopm.2014.41004

Abdollahi E, Abdouss M, Salami-Kalajahi M, Mohammadi A (2016) Molecular recognition ability of molecularly imprinted polymer nano- and micro-particles by reversible addition-fragmentation chain transfer polymerization. Polym Rev 56:557–583. https://doi.org/10.1080/15583724.2015.1119162

Abousalman-Rezvani Z, Eskandari P, Roghani-Mamaqani H, Salami-Kalajahi M (2019a) Synthesis of coumarin-containing multi-responsive CNC-grafted and free copolymers with application in nitrate ion removal from aqueous solutions. Carbohydr Polym 225:115247. https://doi.org/10.1016/j.carbpol.2019.115247

Abousalman-Rezvani Z, Eskandari P, Roghani-Mamaqani H, Mardani H, Salami-Kalajahi M (2019b) Grafting light-, temperature, and CO_2-responsive copolymers from cellulose nanocrystals by atom transfer radical polymerization for adsorption of nitrate ions. Polymer 182: 121830. https://doi.org/10.1016/j.polymer.2019.121830

Ahmad A, Rafatullah M, Sulaiman O, Ibrahim MH, Hashim R (2009) Scavenging behaviour of meranti sawdust in the removal of

methylene blue from aqueous solution. J Hazard Mater 170:357–365. https://doi.org/10.1016/j.jhazmat.2009.04.087

Akkaya MC, Emik S, Güçlü G, İyim TB, Özgümüş S (2009) Removal of basic dyes from aqueous solutions by crosslinked-acrylic acid/acrylamidopropane sulfonic acid hydrogels. J Appl Polym Sci 114:1150–1159. https://doi.org/10.1002/app.30704

Anirudhan TS, Rejeena SR (2012) Poly(acrylic acid)-modified poly(glycidylmethacrylate)-grafted nanocellulose as matrices for the adsorption of lysozyme from aqueous solutions. Chem Eng J 187:150–159. https://doi.org/10.1016/j.cej.2012.01.113

Atta AM, Ismail HS, Elsaaed AM (2012) Application of anionic acrylamide-based hydrogels in the removal of heavy metals from waste water. J Appl Polym Sci 123:2500–2510. https://doi.org/10.1002/app.34798

Balea A, Monte MC, de la Fuente E, Negro C, Blanco Á (2017) Application of cellulose nanofibers to remove water-based flexographic inks from wastewaters. Environ Sci Pollut Res 24:5049–5059. https://doi.org/10.1007/s11356-016-8257-x

Balea A, Monte MC, Fuente E, Sanchez-Salvador JL, Blanco A, Negro C (2019) Cellulose nanofibers and chitosan to remove flexographic inks from wastewaters. Environ Sci Water Res Technol 5:1558–1567. https://doi.org/10.1039/C9EW00434C

Banaei M, Salami-Kalajahi M (2015) Synthesis of poly(2-hydroxyethyl methacrylate)-grafted poly(aminoamide) dendrimers as polymeric nanostructures. Colloid Polym Sci 293:1553–1559. https://doi.org/10.1007/s00396-015-3559-y

Bashir S, Teo YY, Naeem S, Ramesh S, Ramesh K (2017) Correction: pH responsive N-succinyl chitosan/poly(acrylamide-co-acrylic acid) hydrogels and in vitro release of 5-fluorouracil. PLoS One 12:0185505. https://doi.org/10.1371/journal.pone.0179250

Bayramoglu G, Altintas B, Arica MY (2012) Synthesis and characterization of magnetic beads containing aminated fibrous surfaces for removal of reactive green 19 dye: kinetics and thermodynamic parameters. J Chem Technol Biotechnol 87:705–713. https://doi.org/10.1002/jctb.3693

Bekiari V, Sotiropoulou M, Bokias G, Lianos P (2008) Use of poly(N,Ndimethylacrylamide-co-sodium acrylate) hydrogel to extract cationic dyes and metals from water. Colloids Surf A Physicochem Eng Asp 312:214–218. https://doi.org/10.1016/j.colsurfa.2007.06.053

Bidsorkhi HC, Riazi H, Emadzadeh D, Ghanbari M, Matsuura T, Lau WJ, Ismail AF (2016) Preparation and characterization of a novel highly hydrophilic and antifouling polysulfone/nanoporous TiO2 nanocomposite membrane. Nanotechnology 27:415706. https://doi.org/10.1088/0957-4484/27/41/415706

Blus K, Czechowski J, Koziróg A (2014) New eco-friendly method for paper dyeing. Fibres Text East Eur 22:121–125

Bulut Y, Karaer H (2015) Removal of methylene blue from aqueous solution by crosslinked chitosan-g-poly(acrylic acid)/bentonite composite. Chem Eng Commun 202:1635–1644. https://doi.org/10.1080/00986445.2014.968713

Chatterjee S, Tran HN, Godfred OB, Woo SH (2016) Supersorption capacity of anionic dye by newer chitosan hydrogel capsules via green surfactant exchange method. ACS Sustain Chem Eng 6:3604–3614. https://doi.org/10.1021/acssuschemeng.7b03929

Chen H, Wang A (2009) Adsorption characteristics of Cu(II) from aqueous solution onto poly(acrylamide)/attapulgite composite. J Hazard Mater 165:223–231. https://doi.org/10.1016/j.jhazmat.2008.09.097

Chen Y, Liu H, Geng B, Ru J, Cheng C, Zhao Y, Wang L (2017) A reusable surface-quaternized nanocellulose-based hybrid cryogel loaded with N-doped TiO_2 for self-integrated adsorption/photodegradation of methyl orange dye. RSC Adv 7:17279–17288. https://doi.org/10.1039/C7RA00450H

Cheng HL, Feng QH, Liao CA, Liu Y, Wu DB, Wang QG (2016) Removal of methylene blue with hemicellulose/clay hybrid hydrogels. Chin J Polym Sci 34:709–719. https://doi.org/10.1007/s10118-016-1788-2

Ciardelli G, Corsi L, Marcucci M (2001) Membrane separation for wastewater reuse in the textile industry. Resour Conserv Recycl 31:189–197. https://doi.org/10.1016/S0921-3449(00)00079-3

de Paiva SD, da Silva IB, de Moura Santos ECM, Rocha IMV, Martínez-Huitle CA, dos Santos EV (2018) Coupled electrochemical processes for removing dye from soil and water. J Electr Chem Soc 165:E318–E324. https://doi.org/10.1149/2.0391809jes

Dehghani E, Salami-Kalajahi M, Roghani-Mamaqani H (2019) Fabricating cauliflower-like and dumbbell-like Janus particles: loading and simultaneous release of DOX and ibuprofen. Colloids Surf B-Biointerfaces 173:155–163. https://doi.org/10.1016/j.colsurfb.2018.09.068

Dehghani E, Barzgari-Mazgar T, Salami-Kalajahi M, Kahaie-Khosrowshahi A (2020) A pH-controlled approach to fabricate electrolyte/non-electrolyte janus particles with low cytotoxicity as carriers of DOX. Mater Chem Phys 249:123000. https://doi.org/10.1016/j.matchemphys.2020.123000

Fallahi-Sambaran M, Salami-Kalajahi M, Dehghani E, Abbasi F (2018) Investigation of different core-shell toward Janus morphologies by variation of surfactant and feeding composition: a study on the kinetics of DOX release. Colloids Surf B-Biointerfaces 170:578–587. https://doi.org/10.1016/j.colsurfb.2018.06.064

Fallahi-Samberan M, Salami-Kalajahi M, Dehghani E, Abbasi F (2019) Investigating Janus morphology development of poly(acrylic acid)/poly(2-(dimethylamino)ethyl methacrylate) composite particles: an experimental study and mathematical modeling of DOX release. Microchem J 145:492–500. https://doi.org/10.1016/j.microc.2018.11.017

Fang R, He W, Xue H, Chen W (2016) Synthesis and characterization of a high-capacity cationic hydrogel adsorbent and its application in the removal of Acid Black 1 from aqueous solution. React Funct Polym 102:1–10. https://doi.org/10.1016/j.reactfunctpolym.2016.02.013

Gao Q, Zhu Q, Yang CQ (2009) Formation of highly hydrophobic surfaces on cotton and polyester fabrics using silica sol nanoparticles and nonfluorinated alkylsilane. Ind Eng Chem Res 48:9797–9803. https://doi.org/10.1021/ie9005518

García E, Medina R, Lozano M, Hernández Pérez I, Valero M, Franco A (2014) Adsorption of azo-dye orange II from aqueous solutions using a metal-organic framework material: iron-benzenetricarboxylate. Materials 7:8037–8057. https://doi.org/10.3390/ma7128037

Golshan M, Salami-Kalajahi M, Roghani-Mamaqani H, Mohammadi M (2017) Poly(propylene imine) dendrimer-grafted nanocrystalline cellulose: doxorubicin loading and release behavior. Polymer 117:287–294. https://doi.org/10.1016/j.polymer.2017.04.047

Guerra E, Llompart M, Garcia-Jares C (2018) Analysis of dyes in cosmetics: challenges and recent developments. Cosmetics 5:47. https://doi.org/10.3390/cosmetics5030047

Haqani M, Roghani-Mamaqani H, Salami-Kalajahi M (2017) Synthesis of dual-sensitive nanocrystalline cellulose-grafted block copolymers of N-isopropylacrylamide and acrylic acid by reversible addition-fragmentation chain transfer polymerization. Cellulose 24:2241–2254. https://doi.org/10.1007/s10570-017-1249-2

Haque E, Jun JW, Jhung SH (2011) Adsorptive removal of methyl orange and methylene blue from aqueous solution with a metal-organic framework material, iron terephthalate (MOF-235). J Hazard Mater 185:507–511. https://doi.org/10.1016/j.jhazmat.2010.09.035

Hou Z, Zhu W, Song H, Chen P, Yao S (2015) The adsorption behavior and mechanistic investigation of Cr(VI) ions removal by poly(2-(dimethylamino)ethyl methacrylate)/poly(ethylene imine) gels. J Serb Chem Soc 80:889–902. https://doi.org/10.2298/JSC140701024H

Ibrahim SM, El Salmawi KM, Zahran AH (2007) Synthesis of crosslinked superabsorbent carboxymethyl cellulose/acrylamide hydrogels through electron-beam irradiation. J Appl Polym Sci 104:2003–2008. https://doi.org/10.1002/app.25916

Kargarzadeh H, Ahmad I, Abdullah I, Dufresne A, Zainudin SY, Sheltami RM (2012) Effects of hydrolysis conditions on the morphology, crystallinity, and thermal stability of cellulose nanocrystals extracted from kenaf bast fibers. Cellulose 19:855–866. https://doi.org/10.1007/s10570-012-9684-6

Karthika JS, Vishalakshi B (2015) Novel stimuli responsive gellan gum-graft-poly (DMAEMA) hydrogel as adsorbent for anionic dye. Int J Biol Macromol 81:648–655. https://doi.org/10.1016/j.ijbiomac.2015.08.064

Kaşgöz H, Durmus A (2008) Dye removal by a novel hydrogel-clay nanocomposite with enhanced swelling properties. Polym Adv Technol 19:838–845. https://doi.org/10.1002/pat.1045

Khadivi P, Salami-Kalajahi M, Roghani-Mamaqani H (2019a) Evaluation of in vitro cytotoxicity and properties of polydimethylsiloxane-based polyurethane/crystalline nanocellulose bionanocomposites. J Biomed Mater Res A 107:1771–1778. https://doi.org/10.1002/jbm.a.36696

Khadivi P, Salami-Kalajahi M, Roghani-Mamaqani H, Sofla RLM (2019b) Fabrication of microphase-separated polyurethane/cellulose nanocrystal nanocomposites with irregular mechanical and shape memory properties. Appl Phys A Mater Sci Process 125:779. https://doi.org/10.1007/s00339-019-3082-y

Kono H (2015) Preparation and characterization of amphoteric cellulose hydrogels as adsorbents for the anionic dyes in aqueous solutions. Gels 1:94–116. https://doi.org/10.3390/gels1010094

Kono H, Ogasawara K, Kusumoto R, Oshima K, Hashimoto H, Shimizu Y (2016) Cationic cellulose hydrogels cross-linked by poly(ethylene glycol): preparation, molecular dynamics, and adsorption of anionic dyes. Carbohydr Polym 152:170–180. https://doi.org/10.1016/j.carbpol.2016.07.011

Li D, Li Q, Bai N, Dong H, Mao D (2017) One-step synthesis of cationic hydrogel for efficient dye adsorption and its second use for emulsified oil separation. ACS Sustain Chem Eng 5:5598–5607. https://doi.org/10.1021/acssuschemeng.7b01083

Lim LS, Rosli NA, Ahmad I, Mat Lazim A, Mohd Amin MCI (2017) Synthesis and swelling behavior of pH-sensitive semi-IPN superabsorbent hydrogels based on poly(acrylic acid) reinforced with cellulose naonocrystals. Nanomaterials 7:399. https://doi.org/10.3390/nano7110399

Lin Q, Gao M, Chang J, Ma H (2016) Adsorption properties of crosslinking carboxymethyl cellulose grafting dimethyldiallylammonium chloride for cationic and anionic dyes. Carbohydr Polym 151:283–294. https://doi.org/10.1016/j.carbpol.2016.05.064

Liu Y, Zheng Y, Wang A (2010) Enhanced adsorption of Methylene Blue from aqueous solution by chitosan-g-poly (acrylic acid)/vermiculite hydrogel composites. J Environ Sci 22:486–493. https://doi.org/10.1016/S1001-0742(09)60134-0

Liu L, Gao ZY, Su XP, Chen X, Jiang L, Yao JM (2015a) Adsorption removal of dyes from single and binary solutions using a cellulose-based bioadsorbent. ACS Sustain Chem Eng 3:432–442. https://doi.org/10.1021/sc500848m

Liu Y, Wang CF, Chen S (2015b) Facile access to poly (DMAEMA-co-AA) hydrogels via infrared laser-ignited frontal polymerization and their polymerization in the horizontal direction. RSC Adv 5:30514–30521. https://doi.org/10.1039/C5RA01366F

Lu T, Xiang T, Huang XL, Li C, Zhao WF, Zhang Q, Zhao CS (2015) Post-crosslinking towards stimuli-responsive sodium alginate beads for the removal of dye and heavy metals. Carbohydr Polym 133:587–595. https://doi.org/10.1016/j.carbpol.2015.07.048

Luo JH, Li YY, Wang PM, Xia BB, He LP, Yang BW, Jiang B (2017) A facial route for preparation of hydrophobic nano-silica modified by silane coupling agents. Key Eng Mater 727:353–358. https://doi.org/10.4028/www.scientific.net/KEM.727.353

Luo MT, Li HL, Huang C, Zhang HR, Xiong L, Chen XF, Chen XD (2018) Cellulose-based absorbent production from bacterial cellulose and acrylic acid: synthesis and performance. Polymers 10:702. https://doi.org/10.3390/polym10070702

Ma IAW, Shafaamri A, Kasi R, Zaini FN, Balakrishnan V, Subramaniam R, Arof AK (2017) Anticorrosion properties of epoxy/nanocellulose nanocomposite coating. Bioresources 12:2912–2929

Mahmoud NN, Albasha A, Hikmat S, Hamadneh L, Zaza R, Shraideh Z, Khalil EA (2020) Nanoparticle size and chemical modification play a crucial role in the interaction of nano gold with the brain: extent of accumulation and toxicity. Biomater Sci 8:1669–1682. https://doi.org/10.1039/C9BM02072A

Malik PK, Saha SK (2003) Oxidation of direct dyes with hydrogen peroxide using ferrous ion as catalyst. Sep Purif Technol 31:241–250. https://doi.org/10.1016/S1383-5866(02)00200-9

Mazloomi-Rezvani M, Salami-Kalajahi M, Roghani-Mamaqani H, Pirayesh A (2018) Effect of surface modification with different thiol compounds on colloidal stability of gold nanoparticles. Appl Organomet Chem 32:e4079. https://doi.org/10.1002/aoc.4079

Melo BC, Paulino FA, Cardoso VA, Pereira AG, Fajardo AR, Rodrigues FH (2018) Cellulose nanowhiskers improve the methylene blue adsorption capacity of chitosan-g-poly(acrylic acid) hydrogel. Carbohydr Polym 181:358–367. https://doi.org/10.1016/j.carbpol.2017.10.079

Mezohegyi G, van der Zee FP, Font J, Fortuny A, Fabregat A (2012) Towards advanced aqueous dye removal processes: a short review on the versatile role of activated carbon. J Environ Manag 102:148–164. https://doi.org/10.1016/j.jenvman.2012.02.021

Modarresi-Saryazdi SM, Haddadi-Asl V, Salami-Kalajahi M (2018) N, N'-methylenebis(acrylamide)-crosslinked poly(acrylic acid) particles as doxorubicin carriers: a comparison between release behavior of physically loaded drug and conjugated drug via acid-labile hydrazone linkage. J Biomed Mater Res A 106:342–348. https://doi.org/10.1002/jbm.a.36240

Mohammadi M, Salami-Kalajahi M, Roghani-Mamaqani H, Golshan M (2017) Synthesis and investigation of dual pH- and temperature-responsive behaviour of poly[2-(dimethylamino)ethyl methacrylate]-grafted gold nanoparticles. Appl Organomet Chem 31:e3702. https://doi.org/10.1002/aoc.3702

Nikravan G, Haddadi-Asl V, Salami-Kalajahi M (2018) Synthesis of dual temperature– and pH-responsive yolk-shell nanoparticles by conventional etching and new deswelling approaches: DOX release behavior. Colloids Surf B-Biointerfaces 165:1–8. https://doi.org/10.1016/j.colsurfb.2018.02.010

Noein L, Haddadi-Asl V, Salami-Kalajahi M (2017) Grafting of pH-sensitive poly (N, N-dimethylaminoethyl methacrylate-co-2-hydroxyethyl methacrylate) onto halloysite nanotubes via surface-initiated atom transfer radical polymerization for controllable drug release. Int J Polym Mater Polym Biomater 66:123–131. https://doi.org/10.1080/00914037.2016.1190927

Oladipo AA, Gazi M, Saber-Samandari S (2014) Adsorption of anthraquinone dye onto eco-friendly semi-IPN biocomposite hydrogel: equilibrium isotherms, kinetic studies and optimization. J Taiwan Inst Chem Eng 45:653–664. https://doi.org/10.1016/j.jtice.2013.07.013

Panahian P, Salami-Kalajahi M, Hosseini MS (2014a) Synthesis of dual thermoresponsive and pH-sensitive hollow nanospheres by atom transfer radical polymerization. J Polym Res 21:455. https://doi.org/10.1007/s10965-014-0455-y

Panahian P, Salami-Kalajahi M, Hosseini MS (2014b) Synthesis of dual thermosensitive and ph-sensitive hollow nanospheres based on poly(acrylic acid-b-2-hydroxyethyl methacrylate) via an atom transfer reversible addition-fragmentation radical process. Ind Eng Chem Res 53:8079–8086. https://doi.org/10.1021/ie500892b

Panswed J, Wongchaisuwan S (1986) Mechanisms of dye wastewater colour removal by magnesium carbonate-hydrated basic. Water Sci Technol 18:139–144. https://doi.org/10.2166/wst.1986.0045

Patil PS, Phugare SS, Jadhav SB, Jadhav JP (2010) Communal action of microbial cultures for Red HE3B degradation. J Hazard Mater 181: 263–270. https://doi.org/10.1016/j.carbpol.2013.05.093

Pei A, Butchosa N, Berglund LA, Zhou Q (2013) Surface quaternized cellulose nanofibrils with high water absorbency and adsorption capacity for anionic dyes. Soft Matter 9:2047–2055. https://doi.org/10.1039/C2SM27344F

Pyatenko A, Yamaguchi M, Suzuki M (2009) Mechanisms of size reduction of colloidal silver and gold nanoparticles irradiated by Nd:YAG Laser. J Phys Chem C 113:9078–9085. https://doi.org/10.1021/jp808300q

Riazi H, Jalali-Arani A, Taromi FA (2018) In situ synthesis of silica/polyacrylate nanocomposite particles simultaneously bearing carboxylate and sulfonate functionalities via soap-free seeded emulsion polymerization. Mater Chem Phys 207:470–478. https://doi.org/10.1016/j.matchemphys.2018.01.009

Safavi-Mirmahalleh SA, Salami-Kalajahi M, Roghani-Mamaqani H (2019) Effect of surface chemistry and content of nanocrystalline cellulose on removal of methylene blue from wastewater by poly(-acrylic acid)/nanocrystalline cellulose nanocomposite hydrogels. Cellulose 26:5603–5619. https://doi.org/10.1007/s10570-019-02490-1

Salama A, Shukry N, El-Sakhawy M (2015) Carboxymethyl cellulose-g-poly(2-(dimethylamino)ethyl methacrylate) hydrogel as adsorbent for dye removal. Int J Biol Macromol 73:72–75. https://doi.org/10.1016/j.ijbiomac.2014.11.002

Sanchez-Salvador JL, Balea A, Monte MC, Blanco A, Negro C (2018) Study of the reaction mechanism to produce nanocellulose-graft-chitosan polymer. Nanomaterials 8:883. https://doi.org/10.3390/nano8110883

Sarsabili M, Parvini M, Salami-Kalajahi M, Ganjeh-Anzabi P (2013) In situ reversible addition-fragmentation chain transfer polymerization of styrene in the presence of MCM-41 nanoparticles: comparing "Grafting from" and "Grafting through" approaches. Adv Polym Technol 32:21372. https://doi.org/10.1002/adv.21372

Seema HS, Deepika L, Ambika B (2018) A comparative study on discharge printing using conventional and ecological recipe. Trends Textile Eng Fashion Technol 3:TTEFT.000552. https://doi.org/10.31031/TTEFT.2018.03.000552.

Sharifzadeh E, Salami-Kalajahi M, Hosseini MS, Aghjeh MKR (2016) A temperature-controlled method to produce Janus nanoparticles using high internal interface systems: experimental and theoretical approaches. Colloids Surf A Physicochem Eng Asp 506:56–62. https://doi.org/10.1016/j.colsurfa.2016.06.006

Sharma R, Kaith BS, Kalia S, Pathania D, Kumar A, Sharma N, Street RM, Schauer C (2015) Biodegradable and conducting hydrogels based on Guar gum polysaccharide for antibacterial and dye removal applications. J Environ Manag 162:37–45. https://doi.org/10.1016/j.jenvman.2015.07.044

Soleimani K, Tehrani AD, Adeli M (2018) Bioconjugated graphene oxide hydrogel as an effective adsorbent for cationic dyes removal. Ecotoxicol Environ Saf 147:34–42. https://doi.org/10.1016/j.ecoenv.2017.08.021

Stanciu MC, Nichifor M (2019) Adsorption of anionic dyes on a cationic amphiphilic dextran hydrogel: equilibrium, kinetic, and thermodynamic studies. Colloid Polym Sci 297:45–57. https://doi.org/10.1007/s00396-018-4439-z

Tu H, Yu Y, Chen J, Shi X, Zhou J, Deng H, Du Y (2017) Highly cost-effective and high-strength hydrogels as dye adsorbents from natural polymers: chitosan and cellulose. Polym Chem 8:2913–2921. https://doi.org/10.1039/C7PY00223H

Yamada K, Yoshii S, Kumagai S, Fujiwara I, Nishio K, Okuda M, Matsukawa N, Yamashita I (2006) High-density and highly surface selective adsorption of protein–nanoparticle complexes by controlling electrostatic interaction. Japan J Appl Phys 45:4259–4264. https://doi.org/10.1143/JJAP.45.4259

Zhang H, Luan Q, Tang H, Huang F, Zheng M, Deng Q, Xiang X, Yang C, Shi J, Zheng C, Zhou Q (2017) Removal of methyl orange from aqueous solutions by adsorption on cellulose hydrogel assisted with Fe_2O_3 nanoparticles. Cellulose 24:903–914. https://doi.org/10.1007/s10570-016-1129-1

Zhao S, Zhou F, Li L, Cao M, Zuo D, Liu H (2012) Removal of anionic dyes from aqueous solutions by adsorption of chitosan-based semi-IPN hydrogel composites. Compos B Eng 43:1570–1578. https://doi.org/10.1016/j.compositesb.2012.01.015

Zheng X, Li X, Li J, Wang L, Jin W, Pei Y, Tang K (2018) Efficient removal of anionic dye (Congo red) by dialdehyde microfibrillated cellulose/chitosan composite film with significantly improved stability in dye solution. Int J Biol Macromol 107:283–289. https://doi.org/10.1016/j.ijbiomac.2017.08.169

Zhou YM, Zhang M, Wang XH, Huang Q, Min YH, Ma TS, Niu JY (2014) Removal of Crystal Violet by a novel cellulose-based adsorbent: comparison with native cellulose. Ind Eng Chem Res 53: 5498–5506. https://doi.org/10.1021/ie404135y